Trivalent Rare Earth Ion Conduction in the Rare Earth Tungstates with the $Sc_2(WO_4)_3$-Type Structure

Nobuhito Imanaka, Yasuyuki Kobayashi, Kazuyasu Fujiwara, Takuya Asano, Yusuke Okazaki, and Gin-ya Adachi*

Department of Applied Chemistry, Faculty of Engineering, Osaka University, 2-1 Yamadaoka, Suita, Osaka 565-0871, Japan

Received March 12, 1998. Revised Manuscript Received April 27, 1998

To realize a trivalent ion conduction in solids, the $Sc_2(WO_4)_3$-type structure was chosen on the basis of the mobile trivalent ions and the structure which reduces the electrostatic interaction between the framework and the mobile trivalent ionic species as much as possible. The typical conductivity of the rare earth tungstates $R_2(WO_4)_3$ (R = Sc, Y, and Er−Lu) with the $Sc_2(WO_4)_3$-type structure was found to be on the order of 10^{-5} S cm^{-1} at 600 °C. Among the rare earth tungstates, $Sc_2(WO_4)_3$ ($\sigma_{600°C} = 6.5 \times 10^{-5}$ S cm^{-1}, $E_a = 44.1$ kJ mol^{-1}) was found to be the most suitable size for the ionic conduction with regard to the relation between the mobile ion radius and the lattice size. The rare earth ion conducting characteristics were investigated by means of the rare earth concentration cell measurements and dc electrolyses. The electromotive force measurements with the Sc−Y binary alloy and the yttrium tungsten bronze as the electrodes strongly suggest the possibility of the trivalent ion conduction of rare earths such as Sc^{3+} and Y^{3+}. Furthermore, by the dc electrolysis, the mobile species was clarified to be the rare earth ions Sc^{3+} and Y^{3+} in the rare earth tungstates with the $Sc_2(WO_4)_3$-type structure.

Introduction

The ionic conducting species in solid electrolytes is limited to, in most cases, only one species without any electron or hole conduction. Solid electrolytes have peculiar characteristics such as transporting specific ions macroscopically with accompanying electric charge. The current great interest in the solid electrolyte field has been devoted to developing new electrolytes and to seek for their further application.

In general, the ionic mobility in solid electrolytes strongly depends on the valency and ionic size of the mobile ion. The mono- and divalent cationic conductors have the advantage of high ionic conductivity with an associated low activation energy. In contrast, trivalent cations have been regarded to be an extremely poor mobile species for the ionic migration, due to the high electrostatic interaction of the highly charged species with the surrounding framework structure of anions such as O^{2-}. Therefore, only a few papers have reported the possibility of trivalent ion conduction; e.g. Ln^{3+}–β''-alumina,[1−8] β-$LaNb_3O_9$,[9] $LaAl_{11}O_{18}$,[10] and $LaAl_{12}O_{18}N$.[10,11] These papers, however, have only indicated a probability of trivalent cation conduction, and any trivalent ionic conduction in the solids were not directly and quantitatively demonstrated at all.

One approach to realize the trivalent ion conducting solid electrolytes is to select a suitable structure from the stand point of a mobile trivalent ion in solids. In addition, the mobile ion candidates should be able to hold trivalency without varying the valency and have a relatively smaller ionic radius. Compounds with a larger tunnel size, which effectively works to reduce the electrostatic interaction between the mobile ions and framework of the structure as much as possible, possess the proper framework structure. The structure chosen as the most suitable one for the trivalent ion migration was the $Sc_2(WO_4)_3$-type one,[12−16] and aluminum and rare earth ions were selected as the mobile ion candidates. The hexavalent tungsten ion, W^{6+}, which is one of the constituent ions, reduces the interaction between a mobile trivalent ion and constituent oxide ions, since

* To whom all correspondence should be addressed.

(1) Dunn, B.; Farrington, G. C. *Solid State Ionics* **1983**, *9 & 10*, 223.
(2) Carrillo-Cabrera, W.; Thomas, J. O.; Farrington, G. C. *Solid State Ionics* **1983**, *9 & 10*, 245.
(3) Ghosal, B.; Mangle, E. A.; Topp, M. R.; Dunn, B.; Farrington, G. C. *Solid State Ionics* **1983**, *9 & 10*, 273.
(4) Farrington, G. C.; Dunn, B.; Thomas, J. O. *Appl. Phys.* **1983**, *A32*, 159.
(5) Dedecke, T.; Köhler, J.; Tietz, F.; Urland, W. *Eur. J. Solid State Inorg. Chem.* **1996**, *33*, 185.
(6) Köhler, J.; Urland, W.*Solid State Ionics* **1996**, *86−88*, 93.
(7) Köhler, J.; Balzer-Jöllenbeck, G.; Urland, W. *J. Solid State Chem.* **1996**, *122*, 315.
(8) Köhler, J.; Urland, W. *Angew. Chem., Int. Ed. Engl.* **1997**, *36*, 85.
(9) George, A. M.; Virkar, A. N. *J. Phys. Chem. Solids.* **1988**, *49*, 743.
(10) Warner, T. E.; Fray, D. J.; Davies, A. *Solid State Ionics* **1996**, *92*, 99.
(11) Warner, T. E.; Fray, D. J.; Davies, A. *J. Mater. Sci.* **1996**, *32*, 279.
(12) Abrahams, S. C.; Bernstein, J. L. *J. Chem. Phys.* **1966**, *45*, 2745.
(13) Nassau, K.; Levinstein, H. J.; Loiacono, G. M. *J. Phys. Chem. Solids.* **1965**, *26*, 1805.
(14) Borchardt, H. J. *J. Chem. Phys.* **1963**, *39*, 504.
(15) Nassau, K.; Shiever, J. W.; Keve, E. T. *J. Solid State Chem.* **1971**, *3*, 411.
(16) Rode, E. Y.; Lysanova, G. V.; Kuznetsov, V. G.; Gokhman, L. Z. *Russ. J. Inorg. Chem.* **1968**, *13*, 678.

S0897-4756(98)00157-4 CCC: $15.00
Published on Web 06/09/1998

O^{2-} ions in the tungstates are strongly bonded to W^{6+} ions, which hold twice the valency of the trivalent mobile ion. As a result, the trivalent ion is left to migrate in the tungstates smoothly.

Scandium tungstate is isomorphous with the tungstates of trivalent ions such as Gd, Tb, Dy, Ho, Y, Er, Tm, Yb, Lu, In, and Al. A comprehensive study of the electrical transport properties for heavy rare earth tungstates with the $Sc_2(WO_4)_3$-type structure has been done by Verma et al.[17] They concluded that the contribution to the electrical conductivity of the rare earth tungstates is due to the migration of ions or electrons or both. At higher temperatures, the electronic conduction dominates over the ionic conduction, but at lower temperatures, the ionic conduction appears. The mobile ion, however, has not been identified. Recently, we have directly demonstrated conduction of a trivalent ion such as Al^{3+}, Sc^{3+}, Y^{3+}, and Er^{3+} in the tungstate with the $Sc_2(WO_4)_3$-type structure.[18−20]

The aim of the present study is to clarify the individual trivalent species dependencies on both the trivalent ion conducting characteristics and the structure of the trivalent tungstates with the $Sc_2(WO_4)_3$-type structure. The mobile trivalent rare earth ion was identified by using both thermodynamic and kinetic measurements, that is, the rare earth concentration cell, polarization, and electrolysis.

Experimental Section

Sample Preparation. Rare earth tungstates, $R_2(WO_4)_3$ (R = Sc, Y, Er, Tm, Yb, and Lu), were prepared by a conventional solid-state reaction. A stoichiometric amount of R_2O_3 (purity 99.9%) and WO_3 (purity 99.9%) was mixed in a mortar and calcined on a platinum boat at 1000 °C for 12 h in air. The calcined powder was ground and reheated at 1200 °C for 12 h in air. The resulting powder was made into pellets (10 mm in diameter) and sintered at 1300−1400 °C for 12 h in air. In the case of Y and heavy rare earths, Er−Lu, the sample powder was dried in a vacuum at 150 °C before sintering, because they are so hygroscopic at ambient temperature. The procedure for the dense pellet preparation of $Al_2(WO_4)_3$ is the same as described previously.[20]

The samples were characterized by X-ray powder diffractometer and high-temperature X-ray powder diffractometer using Cu Kα radiation (M18XHF, Mac Science). The XRD data were collected by a step-scanning method in the 2θ range from 10° to 120° with a step width of 0.04° and a scan time of 4 s. The XRD patterns obtained were analyzed using the Rietveld refinement program RIETAN-94.[21]

Conducting Property Measurements. Electrical conductivity was measured by an ac and a dc method, using the sintered ceramic pellet with two platinum electrodes in the temperature range from 200 to 900 °C. The ac conductivity measurements were carried out by an ac complex impedance method in the frequency range from 20 Hz to 1 MHz by using Hewlett-Packard precision LCR meter (8284A). The dc conductivity was measured with two platinum electrodes as an ion-blocking electrode. The dc voltage (1 V) was applied between the Pt electrodes sandwiching the sample, and the current passed through the sample was monitored as a function of time in oxygen ($P_{O_2} = 1 \times 10^5$ Pa) and helium ($P_{O_2} = 4$ Pa) atmosphere.

To determine the ionic transference number, t_i, of the sample, the oxygen−air concentration cell measurements as described in eq 1 were performed in the temperature range between 600 and 900 °C.

$$\text{Pt, } O_2\ (P_{O_2} = 1 \times 10^5\ \text{Pa})|R_2(WO_4)_3|\text{air}\ (P_{O_2} = 2.1 \times 10^4\ \text{Pa}),\ \text{Pt} \quad (1)$$

Furthermore, a constant current was passed through the concentration cell, and the terminal voltage was monitored to clarify whether the oxide ion is the conducting species or not.

Rare Earth Concentration Cell. The trivalent ion conduction was investigated by rare earth concentration cell measurements using scandium−yttrium binary alloys and yttrium tungsten bronze as the electrodes.

Sc−Y Binary Alloy. Two types of Sc−Y binary alloys with composition of 10 and 90 mol % Y , $Sc_{90}Y_{10}$ and $Sc_{10}Y_{90}$, were used as electrodes. The alloys were prepared by arc melting the appropriate mixture of scandium and yttrium metals (purity 99.9%) under an argon atmosphere. The arc-melted alloys were remelted at least four times to homogenize the composition. The alloys were annealed at 1000 °C for 50 h in a purified helium atmosphere ($P_{O_2} = 10^{-9}$ Pa) passing through the liquid nitrogen trap. The alloys were cut into thin tablets to use as the electrode (10 mm in diameter). The electromotive force (emf) measurements were carried out with $Sc_2(WO_4)_3$ or $Y_2(WO_4)_3$ as a solid electrolyte by constructing the following cell in a purified helium gas atmosphere at 300 °C:

$$\text{electrode(A) } Sc_{10}Y_{90}|Sc_2(WO_4)_3|Sc_{90}Y_{10}\text{ electrode(B)} \quad (2)$$

$$\text{electrode(A) } Sc_{10}Y_{90}|Y_2(WO_4)_3|Sc_{90}Y_{10}\text{ electrode(B)} \quad (3)$$

The open-circuit voltages were measured using a digital electrometer (R8240, Advantest) with an input impedance of 10^{13} Ω.

Yttrium Tungsten Bronze. Yttrium oxide, tungsten trioxide, and tungsten metal were mixed in the appropriate molar ratio.[22,23] The powder was pelletized and sealed into a quartz tube under 6.7×10^{-2} Pa and was heated for 50 h at 1100 °C. To guarantee its homogeneity, the products were regrounded and reheated several times. All samples were cooled rapidly down to room temperature. The lattice constant of yttrium tungsten bronze, Y_xWO_3 ($x = 0.09$−0.15), was determined by X-ray powder diffraction using high-purity Si powder (purity 99.999%) as an internal standard.

The emf measurements were carried out by constructing the following electrochemical cell with $Y_2(WO_4)_3$:

$$Y_{0.12}WO_3|Y_2(WO_4)_3|Y_xWO_3\ (x = 0.09, 0.10, \text{and } 0.12) \quad (4)$$

Cubic bronzes, Y_xWO_3 ($x = 0.09$−0.12), were used as the electrode, while $Y_{0.12}WO_3$ was fixed for the reference electrode. The cell was heated at 300 °C under a helium gas atmosphere purified by passing through the liquid nitrogen trap.

Electrolysis. The dc electrolysis was performed with two platinum plates as ion-blocking electrodes by applying a direct voltage of 10 V for 250−300 h at 1000 °C in air. After the electrolysis, both the cathodic and anodic surfaces of the samples were analyzed by X-ray microarea diffractometer, scanning electron microscope (SEM, S-800, Hitachi), and electron probe microanalysis (EPMA-1500, Shimadzu). The electrolyzed samples were mounted in a epoxy resin, cut so that the cross-sectional EPMA line analysis could be done from the anode to cathode direction, and then polished with a diamond paste of average diameter 1 μm.

(17) Verma, B. K.; Lal, H. B. *Mater. Res. Bull.* **1981**, *16*, 1579.
(18) Imanaka, N.; Kobayashi, Y.; Adachi, G. *Chem. Lett.* **1995**, 433.
(19) Imanaka, N.; Adachi, G. *J. Alloys Compd.* **1997**, *250*, 492.
(20) Kobayashi, Y.; Egawa, T.; Tamura, S.; Imanaka, N.; Adachi, G. *Chem. Mater.* **1997**, *9*, 1649.
(21) Izumi, F. *The Rietveld Method*; Oxford University Press: Oxford, 1993; Chapter 13.
(22) Ostertag, W. *Inorg. Chem.* **1966**, *5*, 758.
(23) Broyde, B. *Inorg. Chem.* **1967**, *6*, 1588.

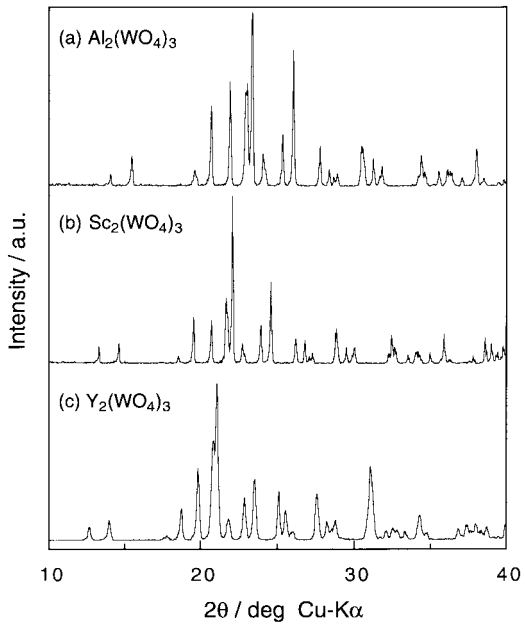

Figure 1. XRD patterns of the trivalent tungstates with the $Sc_2(WO_4)_3$-type structure: (a) $Al_2(WO_4)_3$, (b) $Sc_2(WO_4)_3$, and (c) $Y_2(WO_4)_3$.

Results and Discussion

$Sc_2(WO_4)_3$-Type Structure. The $Sc_2(WO_4)_3$-type structure is orthorhombic with the space group *Pbcn* and is built up with a three-dimensional skeletonal framework of corner-linked ScO_6 octahedra and WO_4 tetrahedra.[12,24] Each ScO_6 octahedron is connected to six WO_4 tetrahedra, while each WO_4 tetrahedron is connected to four ScO_6 octahedra. The basic unit of the network consists of two octahedra and three tetrahedra, $[Sc_2W_3O_{18}]$. These units are linked together via vertexes and connected to form a layer along the *c*-axis. This structure is similar to the frame network of lithium scandium phosphate,[25] γ-$Li_3Sc_2(PO_4)_3$, which has been already reported to be a high lithium ionic conductor. Lithium ions in $Li_3Sc_2(PO_4)_3$ lie in three crystallographic positions and conduct through the opening of the framework consisting of ScO_6 octahedra and PO_4 tetrahedra. Furthermore, the $Sc_2(WO_4)_3$-type structure is closely related to that of the NASICON-type. The framework structure of NASICON is also composed of the unit $[X_2Z_3O_{18}]^{n-}$; each X atom is surrounded with six oxygens situated at vertexes of six ZO_4 tetrahedra, and each Z atom is surrounded by four oxygens situated at vertexes of four XO_6 octahedra.[24] Na^+ ions are capable of conducting through the opening path composed of the three-dimensional framework structure. The main difference between $Sc_2(WO_4)_3$ and the NASICON-type structure is only the arrangement of the basic unit. Therefore, the $Sc_2(WO_4)_3$ structure is expected to possess the unusual feature of a large tunnel size.

The typical X-ray powder diffraction patterns for the samples $R_2(WO_4)_3$ (R = Al, Sc, and Y) at room temperature are shown in Figure 1. The X-ray diffraction analyses for the compounds of Y and Er−Lu were done in a vacuum at room temperature after drying at 150 °C in a vacuum, since they are so hygroscopic.[13] All tungstates were found to be a single phase with an orthorhombic symmetry (space group *Pbcn*), and the XRD patterns of the sample were shifted toward low 2θ with increasing trivalent ionic radius[26] in the tungstates.

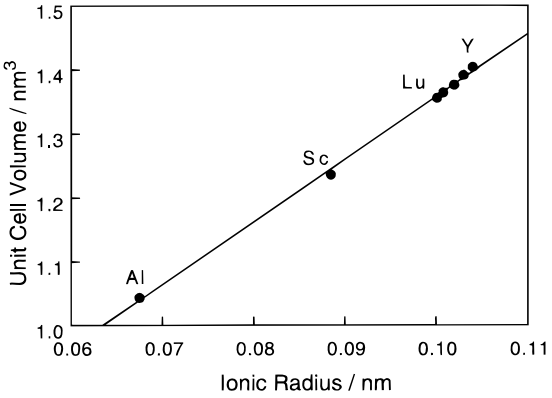

Figure 2. The trivalent ionic radius dependence of the unit cell volume for $M_2(WO_4)_3$.

Table 1. Lattice Parameters and Unit Cell Volume of the Trivalent Tungstates, $M_2(WO_4)_3$

M^{3+}	ionic radius[a]/nm	*a*-axis/nm	*b*-axis/nm	*c*-axis/nm	cell vol/nm^3
Al	0.0675	1.2599	0.9061	0.9141	1.0435
Sc	0.0885	1.3328	0.9586	0.9677	1.2346
Lu	0.1001	1.3781	0.9875	0.9967	1.3564
Yb	0.1008	1.3806	0.9897	0.9988	1.3648
Tm	0.1020	1.3849	0.9924	1.0017	1.3767
Er	0.1030	1.3905	0.9959	1.0049	1.3916
Y	0.1040	1.3954	0.9988	1.0077	1.4045

[a] Six coordinated.[29]

Figure 2 presents the trivalent ionic radius dependencies on the unit cell volume for the tungstate system. The trivalent ionic radius, the lattice parameters, and the unit cell volume refined by the Rietveld method for the trivalent tungstates are summarized in Table 1. The lattice parameters and the cell volume increased upon increasing the trivalent ionic radius. The expansion rate of each lattice parameter toward the trivalent ionic radius was equal and isotropic expansion was observed.

Conducting Properties. The typical complex impedance plot (Cole−Cole plot) for the samples was composed of two kind of components: a semicircle and a line with a 45° slope to the abscissa in the higher and lower frequency region, respectively. In the case of using two types of electrode, Pt or Au, the different behavior was observed in the slope of the line in the lower frequency region. In contrast, no change in the semicircle was recognized. From this result, it becomes clear that the conductivity obtained by an intersecting point of the semicircle in the higher frequency region is identified with the total conductivity of the sintered pellet containing the grain bulk and the grain boundary, similar to the results reported for $Al_2(WO_4)_3$.[20]

The temperature dependencies of the typical electrical conductivity for $M_2(WO_4)_3$ (M = Al, Sc, and Y) are depicted in Figure 3. The temperature dependence of

(24) Piffard, Y.; Verbaere, A.; Kinoshita. M. *J. Solid State Chem.* **1987**, *71*, 121.
(25) Bykov, A. B.; Chipkin, A. P.; Demyanets, L. N.; Doromin, S. N.; Genkina, E. A.; Ivanov-Shits, A. K.; Kondratyuk, I. P.; Maksomov, B. A.; Melnikov, O. K.; Muradyan, L. N.; Simonov, V. I.; Timofeeva, V. A. *Solid State Ionics* **1990**, *38*, 31.
(26) Shannon, R. D. *Acta Crystallogr.* **1976**, *A32*, 751.

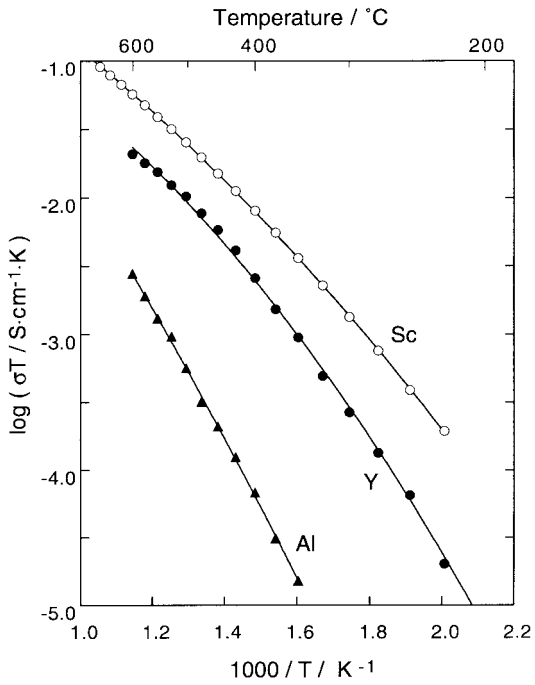

Figure 3. The temperature dependence of the electrical conductivity for $M_2(WO_4)_3$ (M = Al, Sc, and Y).

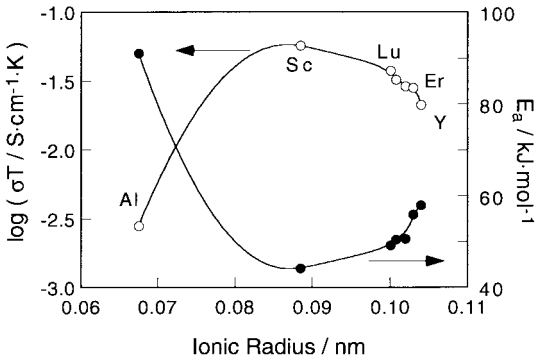

Figure 4. The trivalent ionic radius dependence of the electrical conductivity at 600 °C and the activation energy for $M_2(WO_4)_3$.

the ionic conductivity is usually expressed by the following Arrhenius equation:

$$\sigma T = \sigma_0 \exp(-E_a/RT) \quad (5)$$

where E_a, σ, T, σ_0, and R denote the activation energy, the electrical conductivity, the absolute temperature, the preexponential factor, and the gas constant, respectively. The activation energy (E_a) was calculated from eq 5 in the temperature range from 400 to 600 °C, where the relationship between σT and 1/T is a straight line.

The electrical conductivity at 600 °C and the E_a variation for the tungstates as a function of the trivalent ionic radius is plotted in Figure 4. The conducting properties depend on a kind of trivalent ion in the tungstates, and the most suitable mobile trivalent ion size exists in the trivalent tungstate series with the $Sc_2(WO_4)_3$-type structure. It becomes clear from the figure that $Sc_2(WO_4)_3$ exhibits the highest conductivity, 6.5×10^{-5} S cm^{-1} at 600 °C, and the lowest activation energy, 44.1 kJ mol^{-1}, among the tungstates with the $Sc_2(WO_4)_3$-type structure. In the case of the trivalent ions larger than the most suitable trivalent ion, Sc^{3+}, the electrical conductivity decreased and the activation energy enhanced upon increasing the ionic radius. This is because the increasing ratio of the ionic size is larger than that of the lattice size. In contrast, for the smallest ion, Al^{3+}, the conductivity was the lowest and the activation energy was the highest in the tungstate series. The extremely poor migration of Al^{3+} in the $Sc_2(WO_4)_3$-type structure is due to the high electrostatic interaction caused by its low polarizability, with surrounding anions composing the skeleton structure.

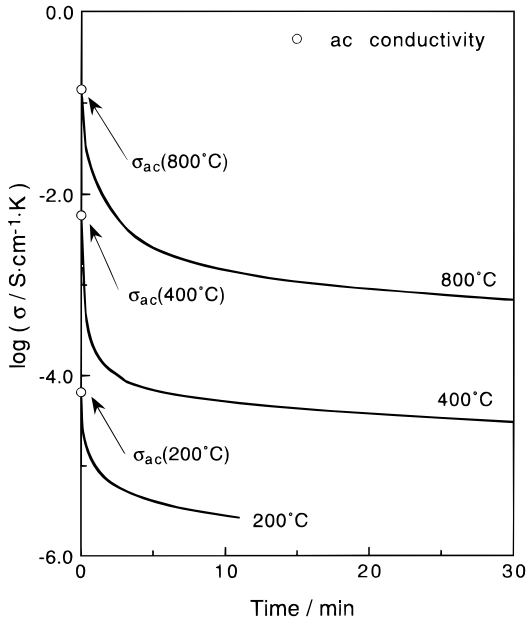

Figure 5. The ac conductivity (○) and the time dependence of the dc conductivity for $Sc_2(WO_4)_3$ in air.

To investigate the electrical conducting properties of the rare earth tungstates, the dc conductivity was measured as a function of time and compared with the ac one. Figure 5 shows the time dependencies of the dc conductivity at the various temperatures in air for $Sc_2(WO_4)_3$, which shows the highest electrical conductivity among the trivalent tungstates, as well as the data of the ac conductivity. The dc conductivities were found to decrease abruptly compared with the ac conductivities and approached a steady current. The dc conductivities were 2−3 orders of magnitudes lower than ac ones in the whole temperature region measured. These polarization phenomena suggest that the main conducting species is neither an electron nor a hole but only an ion and that the ionic transference number is expected to be over 0.99 for scandium tungstate.

To examine the possibility of O^{2-} conduction, the dc conductivity was measured at 700 °C in two different atmospheres: O_2 ($P_{O_2} = 10^5$ Pa) and He ($P_{O_2} = 4$ Pa). A clear polarization behavior, that the ratio of dc to ac conductivity (σ_{dc}/σ_{ac}) abruptly decreased from unity, was observed in both atmospheres. If an O^{2-} ion is the predominant mobile ionic species, a clear polarization would be observed in the helium atmosphere, while in the oxygen atmosphere the dc conductivity would be the same as that obtained by ac method and no polarization behavior would be observed, as described in ref 20. Having the same polarization in the two atmospheres, therefore, reveals that the oxide ion is eliminated as a candidate for the mobile ionic species.

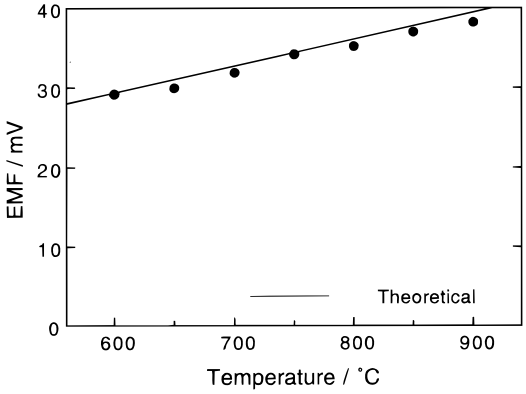

Figure 6. The temperature dependence of the electromotive force (emf) for $Sc_2(WO_4)_3$ of the oxygen−air concentration cell. The straight line shows the theoretical emf.

Furthermore, the ionic transference number, t_i, was investigated by constructing the oxygen−air concentration cell and compared with the result obtained by the polarization measurements. The theoretical emf values of the cell were calculated from the following Nernst equation:

$$E = -\frac{RT}{4F} \ln \frac{P_{O_2(II)}}{P_{O_2(I)}} \qquad (6)$$

where F is the Faraday constant. The measured and theoretical emf values coincided well in the temperature range from 600 to 900 °C, as presented in Figure 6 and the t_i was estimated to be unity and identical to the t_i value of over 0.99 from the polarization measurements. In the case of the oxide ion conductor, it is possible to draw a constant current from the concentration cell. By drawing the current, the terminal voltage between the sample appreciably decreased and a steady current could not be derived. Therefore, it can be easily elucidated from this phenomenon that the oxide ion is not a conducting species in the rare earth tungstate. This also supports the result obtained from the polarization analysis described above.

Rare Earth Concentration Cell. *Sc−Y Binary Alloy*. The scandium or yttrium concentration cell measurements were performed using Sc−Y alloy[27] electrodes of two different compositions, $Sc_{90}Y_{10}$ and $Sc_{10}Y_{90}$, with $Sc_2(WO_4)_3$ or $Y_2(WO_4)_3$, which were considered to be a Sc^{3+} or a Y^{3+} conductor, respectively. In the case of the Sc^{3+} ion conductor, Sc^{3+} ions would be transported from the electrode B $Sc_{90}Y_{10}$ to the electrode A $Sc_{10}Y_{90}$, since the scandium activity at electrode B is higher than that at electrode A in the concentration cell (eq 2). On the other hand, in the cell in eq 3, Y^{3+} ions diffuse into the opposite direction of cell 2 and cell 3 generates the reversed emf toward cell 2. In the case of $Sc_2(WO_4)_3$, the emf obtained with cell 2 was around 20 mV. In contrast to this, when $Y_2(WO_4)_3$ was set for $Sc_2(WO_4)_3$, the emf that appeared with cell 3 was about −20 mV. The emf outputs of the cell with $Sc_2(WO_4)_3$ and $Y_2(WO_4)_3$ were closely related to the difference in Sc and Y activity, respectively. This phenomena strongly suggest that the conducting species is neither an electron nor a hole and that the mobile species is strongly expected to be the Sc^{3+} and Y^{3+} ion in $Sc_2(WO_4)_3$ and $Y_2(WO_4)_3$, respectively.

(27) Masslski, T. B. *Binary Alloy Phase Diagrams*; American Society of Metals: Metals Park, OH, 1986; p 2037.

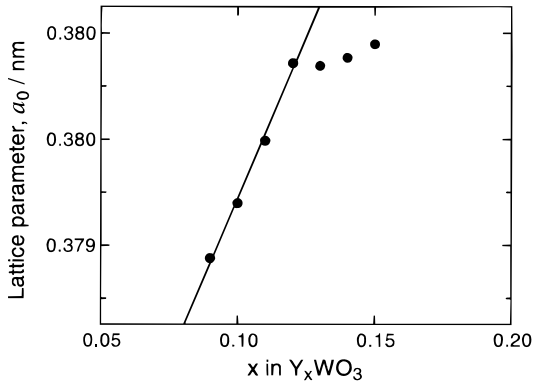

Figure 7. The composition dependence of the cubic cell parameter, a_0, for yttrium tungsten bronze, Y_xWO_3 ($x = 0.09$−0.15).

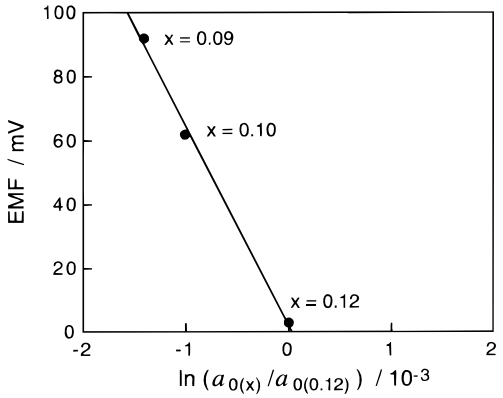

Figure 8. The relationship between emf obtained by the yttrium concentration cell (eq 4) and $\ln(a_{0(x)}/a_{0(0.12)})$ ($x = 0.09$, 0.10, and 0.12).

Yttrium Tungsten Bronze. Tungsten bronzes containing the rare earth have been already reported[22,23] and it was clarified that scandium does not form a tungsten bronze. Y and lanthanoid tungsten bronzes exist in a tetragonal form and a cubic perovskite-type structure at lower and higher concentration of the rare earth, respectively. In the case of yttrium, below $x = 0.09$ a tetragonal form appears and above $x = 0.15$ two additional phase, $Y_2(WO_4)_3$ and WO_2, are present. The yttrium tungsten bronzes Y_xWO_3 ($x = 0.09$−0.15) obtained were a blue-violet powder and were found to be a single cubic phase from XRD measurements. The cubic lattice parameter, a_0, of the yttrium tungsten bronzes obtained linearly increased with the yttrium content when x is between 0.09 and 0.12, as shown in Figure 7. Above $x = 0.12$, a_0 was constant as the yttrium content increased. Therefore, a homogeneous cubic perovskite-type structure is found for Y_xWO_3 when x is between 0.09 and 0.12.

The yttrium concentration cell was constructed by using three types of tungsten bronzes, $x = 0.09$, 0.10, and 0.12, which have a cubic phase. $Y_{0.12}WO_3$ was used as the reference electrode. The emf values for the cell with $Y_{0.12}WO_3$ | $Y_2(WO_4)_3$ | $Y_{0.09}WO_3$, $Y_{0.12}WO_3$ | $Y_2(WO_4)_3$ | $Y_{0.10}WO_3$, and $Y_{0.12}WO_3$ | $Y_2(WO_4)_3$ | $Y_{0.12}WO_3$ system were steady at 92, 62, and 3 mV, respectively.

Structural, electrical, and thermodynamic properties have been precisely investigated with respect to sodium

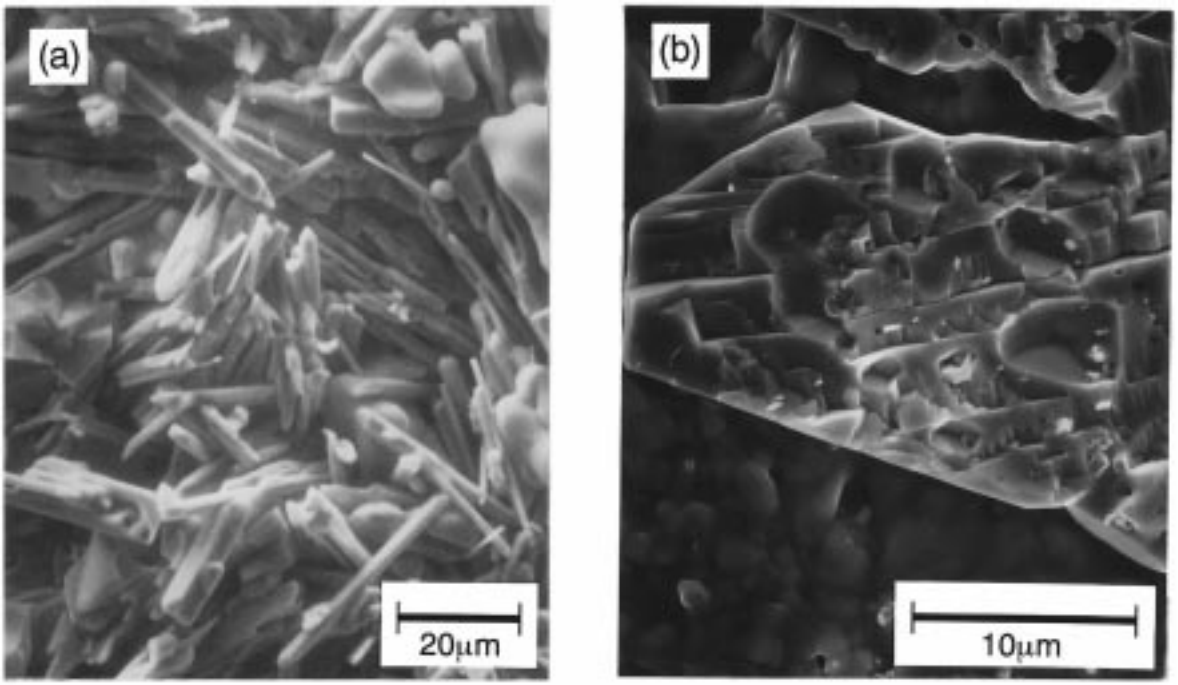

Figure 9. SEM photographs of the (a) cathodic and (b) anodic surfaces of $Sc_2(WO_4)_3$ after the electrolysis.

tungsten bronze. The tungsten bronze, M_xWO_3, shows the metallic conduction because of a mixed valency state of W^{5+}/W^{6+}, while it exhibits the ionic conduction due to M^{n+} ion diffusion. Therefore, sodium tungsten bronze is applicable as a Na^+ reversible electrode for measuring the conductivity of the Na^+ ion conductor.[28] The Na activity in the sodium tungsten bronze Na_xWO_3 has been measured using an electrochemical cell with Pyrex as a solid electrolyte and reported to be directly proportional to sodium concentration in the cubic phase region.[29] The Y activity in yttrium tungsten bronze is not known yet. However, in the Y_xWO_3 system, the yttrium activity is expected to be directly related to the yttrium concentration in a cubic bronze, Y_xWO_3, with x between 0.09 and 0.12. Therefore, the relation between the emf vs lattice parameter was examined here

$$E=-\frac{RT}{3F}\ln\frac{a_{Y(x)}}{a_{Y(0.12)}}\propto\ln\frac{a_{0(x)}}{a_{0(0.12)}} \qquad (7)$$

where a_o and a_Y are the lattice parameter and the yttrium activity in the yttrium tungsten bronzes, respectively. Figure 8 shows the relationship between the measured EMF and $\ln(a_{0(x)}/a_{0(0.12)})$ ($x = 0.09$, 0.10, and 0.12). The emf values obtained by the yttrium concentration cell (eq 4) were proportional to the logarithm of the cubic lattice parameter ratio of Y_xWO_3 and were found to follow the Nernst equation (7). This indicates that $Y_2(WO_4)_3$ is a Y^{3+} pure ionic conductor.

Electrolysis. To directly determine the mobile ionic species in the rare earth tungstates, an electrolysis was carried out by sandwiching the tungstate between two platinum electrodes. Here, the tungstate that showed the highest conductivity was selected, $Sc_2(WO_4)_3$. The

Table 2. Scandium and Tungsten Content of the Bulk before the Electrolysis and Those of the Deposits on Cathodic and Anodic Bulk Surface for $Sc_2(WO_4)_3$ after the Electrolysis

		content/atom %	
	shape	Sc	W
bulk		39.7	61.9
cathode	needlelike	84.3	15.7
anode	platelike		100

SEM photographs of the cathodic and anodic bulk surfaces of $Sc_2(WO_4)_3$ after the electrolysis were presented in Figure 9. Many needle-shaped deposits were observed on the cathodic surface (panel a). In contrast, the color of the anodic surface of the sample changed from white before the electrolysis to yellow after the electrolysis and plate-shaped deposits were observed by SEM (panel b). From EPMA measurements, it was found that the needle-shaped deposits contained scandium and tungsten and that the ratio of the scandium to tungsten element in the deposits considerably increased to about 6:1 compared with that of the tungstate bulk (2:3) before the electrolysis (see Table 2). On the other hand, the plate-shaped deposits that appeared on the anodic surface were found to contain only tungsten. Figure 10 shows the X-ray microarea diffraction patterns of the surface after and before the electrolysis for $Sc_2(WO_4)_3$. The deposits on cathodic and anodic surface after the electrolysis were identified as Sc_6WO_{12} and WO_3, respectively. The ratio of composition of the deposits on cathodic surface was in exact agreement with that measured by EPMA. It was clearly shown that the element Sc was segregated on the cathodic surface after the electrolysis.

The cross-sectional EPMA line analysis for $Sc_2(WO_4)_3$ after the electrolysis is presented in Figure 11. The profile of Sc showed a large segregation of the element Sc at the cathodic surface of the electrolyte, while W was almost flat in the all region, except for at the

(28) Whittingham, M. S.; Huggins, R. A. *J. Chem Phys.* **1971**, *29*, 429.
(29) Ramanarayanan, T. A.; Worrell, W. L. *J. Electrochem. Soc.* **1974**, *121*, 1530.

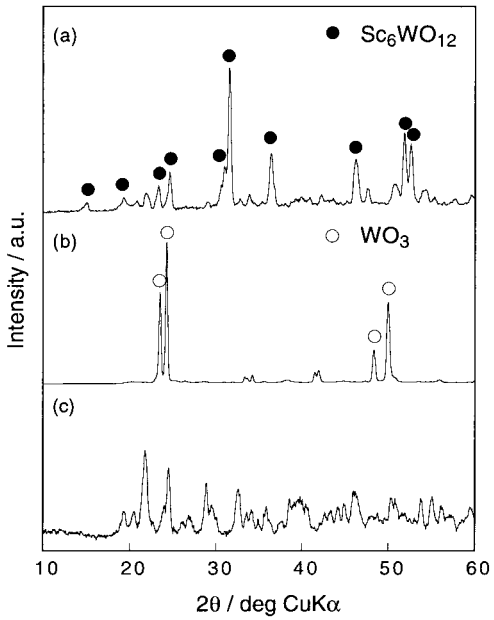

Figure 10. X-ray microarea diffraction patterns of the (a) cathode and (b) anode deposits after the electrolysis, and (c) the bulk surface before the electrolysis for $Sc_2(WO_4)_3$.

cathodic side where W decreased due to the deposition of scandium. These behaviors strongly suggest that trivalent Sc^{3+} ion migrates from anode to cathode and that the scandium segregation occurs on the cathodic surface, while tungsten oxide is left on the anodic surface. The same result was obtained for $Y_2(WO_4)_3$ also. These results clearly indicate that the trivalent rare earth ions Sc^{3+} and Y^{3+} in the $Sc_2(WO_4)_3$-type structure are the predominant mobile ionic species in the tungstates.

Conclusion

The $Sc_2(WO_4)_3$-type structure was selected upon considering both the mobile trivalent ions and the structure which reduces as much as possible the electrostatic interaction between the mobile trivalent ionic species and the framework of the structure. By the electromotive force measurements and by the dc electrolysis, the mobile ion species in the $Sc_2(WO_4)_3$-type structure was clearly demonstrated to be the trivalent rare earth ions of Sc^{3+} and Y^{3+} in the rare earth tungstates.

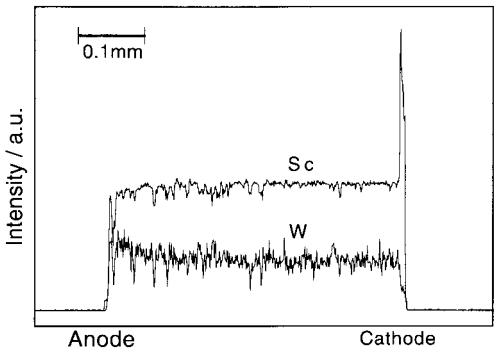

Figure 11. Cross-sectional EPMA line analysis of scandium and tungsten element for the $Sc_2(WO_4)_3$ pellet after the electrolysis.

Acknowledgment. We thank Dr. K. Yamada for the EPMA measurements and Dr. K. Toda for the Rietveld analysis. The present work was partially supported by a Grant-in-Aid for Scientific Research No. 09215223 on Priority Areas (No. 260), Nos. 06241106, 06241107, and 093065 from The Ministry of Education, Science, Sports and Culture. One of the authors (Y.K.) is the Fellowship member of the Japan Society for the Promotion of Science for Japanese Junior Scientists. This work was also supported by the "Research for the Future, Preparation and Application of Newly Designed Solid Electrolytes (JSPS-RFTF96P00102)" Program from the Japan Society for the Promotion of Science.

CM980157E